Coevolution of Patch Selection in Stochastic Environments

Sebastian J. Schreiber,1,* Alexandru Hening,2 and Dang H. Nguyen3

Department of Evolution and Ecology, University of California, Davis, California 95616;
 Department of Mathematics, Texas A&M University, College Station, Texas 77843;
 Department of Mathematics, University of Alabama, Tuscaloosa, Alabama 35487
 Submitted March 17, 2022; Accepted December 2, 2022; Electronically published June 29, 2023
 Online enhancements: supplemental PDF.

ABSTRACT: Species interact in landscapes where environmental conditions vary in time and space. This variability impacts how species select habitat patches. Under equilibrium conditions, evolution of this patch selection can result in ideal free distributions where per capita growth rates are zero in occupied patches and negative in unoccupied patches. These ideal free distributions, however, do not explain why species occupy sink patches, why competitors have overlapping spatial ranges, or why predators avoid highly productive patches. To understand these patterns, we solve for coevolutionarily stable strategies (coESSs) of patch selection for multispecies stochastic Lotka-Volterra models accounting for spatial and temporal heterogeneity. In occupied patches at the coESS, we show that the differences between the local contributions to the mean and the variance of the long-term population growth rate are equalized. Applying this characterization to models of antagonistic interactions reveals that environmental stochasticity can partially exorcize the ghost of competition past, select for new forms of enemy-free and victimless space, and generate hydra effects over evolutionary timescales. Viewing our results through the economic lens of modern portfolio theory highlights why the coESS for patch selection is often a bet-hedging strategy coupling stochastic sink populations. Our results highlight how environmental stochasticity can reverse or amplify evolutionary outcomes as a result of species interactions or spatial heterogeneity.

Keywords: coevolution, habitat selection, environmental stochasticity, portfolio theory, evolutionarily stable strategy.

Introduction

Evolution of habitat choice plays a key role in shaping the distribution and abundance of species. Evolutionary drivers of this choice include spatial and temporal variation in abiotic conditions among habitat patches and species interactions within habitat patches. One successful theoretical approach to evaluate the relative importance of these drivers assumes that individuals can freely chose their habitat patches with no costs to dispersal (Fretwell and Lucas 1969; Rosenzweig 1981, 1991; Holt 1997; Morris 2003; Křivan et al. 2008; Morris 2011). Under equilibrium con-

ditions, this theoretical approach provides empirically supported predictions about the spatial distributions of predators and their prey (Oksanen et al. 1995; Schreiber et al. 2000) and competing species (Lawlor and Maynard Smith 1976; Diamond 1978; Connell 1980). In temporally variable environments, this approach also provides an evolutionary explanation of why populations occupy habitat patches where deaths exceed births (Holt 1997; Jansen and Yoshimura 1998; Schreiber 2012). Despite these significant advances, there is not a comprehensive approach for how temporal variation, spatial heterogeneity, and species interactions simultaneously drive the coevolution of habitat choices. Here, we introduce one such framework.

When individuals select habitat patches to maximize their fitness, theory predicts that the population will reach an ideal free distribution in which the per capita growth rates are equal in all of the occupied patches and lower in the unoccupied patches (Fretwell and Lucas 1969; Křivan et al. 2008). Two classical concepts, enemy-free space and the ghost of competition past, from evolutionary ecology follow from this ideal free theory. Jeffries and Lawton (1984) defined enemy-free space as "ways of living that reduce or eliminate a species' vulnerability to one or more species of natural enemies" (p. 269). In a spatial context, enemy-free space corresponds to a species living in habitat patches where there are fewer or no natural enemies, a phenomenon that has been observed in several empirical systems (Denno et al. 1990; Fox and Eisenbach 1992; Berdegue et al. 1996; Murphy 2004; Cole et al. 2005; Heisswolf et al. 2005; Kaminski et al. 2010; Roy et al. 2011; Murphy et al. 2014; Greeney et al. 2015). Ideal free distributions of predators and their prey yield enemy-free space when patches of lower quality for the prey are also lower quality for the predator (Schreiber et al. 2000; Schreiber and Vejdani 2006). Consistent with these theoretical predictions, Fox and Eisenbach (1992) found that diamondback moths (Plutella xylostella) preferentially laid eggs on collards and red cabbage grown on low-fertilized soils while its main

^{*} Corresponding author; email: sschreiber@ucdavis.edu.

parasitoid, an ichneumonid wasp (*Diadegma insulare*), preferentially searched for hosts on collards grown on high-fertilized soils. These contrary choices occurred despite diamondback moth larvae, in the absence of the wasps, having higher survival rates and growing to larger sizes on host plants from high-fertilized soils.

For competing species, ideal free theory predicts that eventually competitors never occupy the same habitat patch. At equilibrium, each species occupies only patches in which it is competitively superior (Lawlor and Maynard Smith 1976). As competitive interactions from the past led to habitat choices eliminating competition in the present, this outcome is known as "the ghost of competition past" (Connell 1980). Such a haunting may explain the spatial distribution of two Crateroscelis warblers species in New Guinea (Diamond 1973, 1978), where one species abruptly replaces the other at an altitude of 1,643 m. Despite this sharp transition in warblers, shifts in abundance of competing species typically are more gradual with substantive regions of overlap (Noon 1981; Chettri and Acharya 2010; Campos-Cerqueira et al. 2017; Burner et al. 2019). Along these regions of overlap, each competitor may shift from living in source patches (e.g., where it is competitively dominant) to living in sink patches (e.g., where it is competitively inferior; Amarasekare and Nisbet 2001).

Under equilibrium conditions, ideal free theory predicts that birth rates equal death rates in occupied patches. Consequently, there can be no sink populations—local populations whose death rates exceed their birth rates (Holt 1985; Pulliam 1988; Pulliam and Danielson 1991). Nonetheless, sink populations have been observed in many taxonomic groups, including birds (Dias et al. 1996; Vierling 2000; Keagy et al. 2005; Tittler et al. 2006), plants (Kadmon and Tielbörger 1999), mammals (Kreuzer and Huntly 2003; Robinson et al. 2008; Monson et al. 2011), reptiles (Manier and Arnold 2005), amphibians (Rowe et al. 2001), and fishes (Hänfling and Weetman 2006; Barson et al. 2009; McDowall 2010). Indeed, a meta-analysis of 90 source-sink assessments found that 60% of the studied populations were identified as sink populations (Furrer and Pasinelli 2016). These sink populations can be either unconditional or conditional sink populations (Loreau et al. 2013). Unconditional sink populations have negative per capita growth rates in the absence of conspecific and antagonistic interactions. Alternatively, conditional sink populations have negative per capita growth rates due to high densities of conspecifics (Watkinson and Sutherland 1995), heterospecific competitors (Amarasekare and Nisbet 2001), or predators (Holt 1977).

Patch selection theory for single-species models suggests that unconditional sink populations may evolve in temporally variable environments (Holt 1997; Jansen and Yoshimura 1998; Schmidt et al. 2000; Jonzén et al. 2004; Schreiber 2012). Intuitively, making use of low-quality but environ-

mentally stable patches can buffer populations against environmental fluctuations in patches that, on average, are of higher quality (Cohen 1966; Holt 1997; Jansen and Yoshimura 1998; Kisdi 2002; Schreiber 2012). However, whether this evolutionary explanation also extends to sink populations in a community context remains largely unexplored. A notable exception is the work of Schmidt et al. (2000), who studied the evolution of patch choice for two competing species in a fluctuating environment with two habitat patches. They found that these environmental fluctuations can result in patches being occupied by both competitors and thereby partially exorcize the ghost of competition past. However, to what extent these conclusions apply to more than two competing species (or other forms of species interactions) or landscapes of greater complexity is unknown.

Here, we introduce a framework for analyzing the coevolution of patch selection for multispecies communities in spatially and temporally heterogeneous environments. The framework involves stochastic counterparts of the general Lotka-Volterra models that have been a mainstay of theoretical work in community ecology (May 1975; Holt 1977; Polis and Holt 1992; Law and Morton 1996; Chesson and Kuang 2008; Edwards and Schreiber 2010; Rohr et al. 2016; Schreiber et al. 2018). For these models, we explore coevolutionarily stable strategies (coESSs) for patch selection whereby each species has its own patch selection strategy and any subpopulation playing a different strategy fails to establish (Roughgarden 1979; Brown and Vincent 1987; Foster and Young 1990; Rand et al. 1994; Feng et al. 2022). Using an analytically tractable characterization of the coESSs, we examine several questions. First, for species playing the coESS for patch selection, we ask: Is there any demographic quantity that is equal in all occupied patches? We provide a positive answer to this question and thereby extend earlier work on single-species models (Schreiber 2012; Evans et al. 2015). Second, when do sink population evolve? In particular, as earlier theory only considered single-species models (Holt 1997; Jansen and Yoshimura 1998; Schreiber 2012; Evans et al. 2015), when do species interactions result in the evolution of conditional versus unconditional sink populations? Finally, in what ways does environmental stochasticity exorcize the ghost of competition past, and in what ways does it amplify or dampen the evolution of enemy-free space? Collectively, the answers to these questions highlight the interactive effects of spatial heterogeneity, temporal variation, and species interactions on the evolution of habitat choice.

Models and Methods

We model a community of n species living in an environment with k patches. These patches may represent distinct habitats, patches of the same habitat type, or combinations

thereof. The dynamics within a patch are modeled by stochastic Lotka-Volterra differential equations (May 1973, 1975; Turelli 1977, 1978; Turelli and Gillespie 1980; Turelli 1986; Lande et al. 2003; Schreiber et al. 2011; Evans et al. 2013, 2015; Nolting and Abbott 2016; Hening and Nguyen 2018b, 2018c; Hening et al. 2021). To couple these local dynamics, we do not explicitly model movement, but instead we assume that each species has a fixed fraction of its population in each of these patches. We call this fixed spatial distribution for a species its "patch selection strategy." This strategy may correspond to freely dispersing individuals spending a fixed fraction of time in each patch or allocating a fixed fraction of their offspring to a patch (Holt 1997; Jansen and Yoshimura 1998; Schmidt et al. 2000; Bascompte et al. 2002; Schreiber 2012; Evans et al. 2015). The resulting models are a multispecies version of the models introduced in Schreiber (2012).

We introduce a definition of coESS of patch selection. Our definition merges the concepts of coESS for deterministic models (Roughgarden 1979; Brown and Vincent 1987; Rand et al. 1994) and ESS for single-species stochastic models (Foster and Young 1990; Feng et al. 2022). Roughly, coevolutionary stability requires that any small population of a species playing a different strategy from the rest of its population will not establish. Using invasion growth rates of mutant strategies, we provide both analytical and numerical approaches for computing the coESS.

The Models

Within-Patch Dynamics. Consider one patch in the landscape, say, patch ℓ . For the moment, assume that all species use only this patch; that is, the patch selection strategy of each species i is to have 100% of individuals use patch ℓ . To model the dynamics of species i within this patch, let $x_i^{\ell}(t)$ denote its density at time t, b_i^{ℓ} its intrinsic per capita growth rate in the absence of other species, and a_{ii}^{ℓ} its per capita interaction rate with species j. These quantities determine the deterministic forces acting on species i. Specifically, the change $\Delta x_i^{\ell}(t) = x_i^{\ell}(t + \Delta t) - x_i^{\ell}(t)$ in the density of species i over a small time step Δt satisfies

$$\mathbb{E}[\Delta x_i^{\ell}(t)|x^{\ell}(t)] \approx x_i^{\ell}(t) \left(\sum_{j=1}^n a_{ij}^{\ell} x_j^{\ell}(t) + b_i^{\ell}\right) \Delta t, \tag{1}$$

where $x^{\ell} = (x_1^{\ell}(t), \dots, x_n^{\ell}(t))$ is the community state in patch ℓ at time t and $\mathbb{E}[X|Y]$ denotes the conditional expectation of a random variable X with respect to the random variable Y. Thus, the expected instantaneous change of the species density is given by a Lotka-Volterra model.

To capture the role of environmental stochasticity, we assume that the variance in the growth of species i in patch ℓ over a time interval Δt satisfies

$$\operatorname{Var}[\Delta x_i^{\ell}(t)|x^{\ell}(t)] \approx \sigma_i^{\ell\ell}(x_i^{\ell}(t))^2 \Delta t$$

where Var[X|Y] denotes the conditional variance of X with respect to Y. Taking the limit as Δt gets infinitesimally small, the population dynamics when all individuals use only patch ℓ are given by the following Itô stochastic differential equations (Gardiner 2009; Oksendal 2013):

$$dx_{i}^{\ell}(t) = x_{i}^{\ell}(t) \left(\left(\sum_{j=1}^{n} a_{ij}^{\ell} x_{j}^{\ell}(t) + b_{i}^{\ell} \right) dt + dE_{i}^{\ell}(t) \right),$$

$$i = 1, 2, ..., n,$$
(2)

where $E_i^{\ell}(t)$ is a (nonstandard) Brownian motion with mean 0 and variance $\sigma_i^{\ell\ell}$ (for how to represent $E_i(t)$ as a linear combination of standard Brownian motions, see the supplemental PDF, sec. S1). One can interpret equation (2) as approximately updating densities by Lotka-Volterra dynamics plus multiplicative, normally distributed noise that corresponds to fluctuations in the intrinsic rates of growth.

Global Dynamics. To describe the global dynamics when species use more than one patch, let p_i^{ℓ} denote the fraction of individuals of species i selecting patch ℓ and $\vec{p}_i =$ $(p_i^1, p_i^2, ..., p_i^k)$ denote the patch selection strategy of species *i*; for example, if $\vec{p}_1 = (0.5, 0.3, 0.2)$, then there are k = 3 patches, and at any point in time 50% of individuals of species 1 are using patch 1, 30% are using patch 2, and 20% are using patch 3. If x_i denotes the global density of species *i*, then $x_i^{\ell} = p_i^{\ell} x_i$ is the density of species *i* in patch ℓ . Let $P = (\vec{p}_1 \vec{p}_2 \dots \vec{p}_k)$ denote the matrix of the patch selection strategies for all species where the ith column of P corresponds to the patch selection strategy of species i.

To account for spatial correlations in the environmental fluctuations across the patches, we assume that the per capita growth rates of species i in patches ℓ and m over a time interval of length Δt satisfy

$$Cov[\Delta x_i^{\ell}(t), \Delta x_i^{m}(t)|x^{\ell}(t), x^{m}(t)] \approx \sigma_i^{\ell m} x_i^{\ell}(t) x_i^{m}(t) \Delta t,$$

where Cov[X, Y|Z, W] denotes the covariance between random variables X and Y given the random variables Zand W. The covariance matrix $\sum_{i} = (\sigma_{i}^{\ell m})_{\ell,m}$ for species i captures the spatial dependence between the temporal fluctuations in intrinsic growth rates across patches.

Under these assumptions, the community dynamics of the n species interacting in the k patches are given by the following system of Itô stochastic differential equations:

$$dx_{i}(t) = x_{i}(t) \sum_{\ell=1}^{k} p_{i}^{\ell} \left(\left(\sum_{j=1}^{n} (a_{ij}^{\ell} p_{j}^{\ell} x_{j}(t) + b_{i}^{\ell}) dt + dE_{i}^{\ell}(t) \right),$$

$$i = 1, 2, \dots, n,$$
(2)

where for species $i, \vec{E}_i(t) = (E_i^1(t), ..., E_i^k(t))$ is a multivariate Brownian motion with covariance matrix \sum_{i} . We make no assumptions about the cross correlations, $\sigma_{ij}^{\ell m} := \text{Cor}[E_i^{\ell}(t), E_j^m(t)]$, in the environmental fluctuations experienced by different species $i \neq j$.

Methods

To study coevolution of patch selection strategies, we introduce several methods. First, we characterize the mean densities of the species at stationary distributions for the community. Second, we introduce a definition of a coESS that accounts for environmental stochasticity. Finally, we describe a numerical method for solving for these coESSs.

Stationary Distributions and Stochastic Growth Rates. To study the coevolution of patch selection strategies, we need to identify when species coexist. Criteria for determining coexistence for stochastic Lotka-Volterra models were developed by Hening and Nguyen (2018a) and Hening et al. (2021), complementing earlier work for discrete-time models and continuous-time replicator equations (Schreiber et al. 2011; Benaïm and Schreiber 2019). These criteria are based on invasion growth rates, the long-term average growth rates of species when rare (see the supplemental PDF, sec. S1). Importantly, these invasion-based criteria ensure that the statistical properties of the coexisting species' densities are characterized by a unique stationary distribution (depending on P). When the patch selection strategies of the species are $P = (\vec{p}_1, ..., \vec{p}_k)$, let $\hat{x}_i(P)$ be the mean density of species *i* at this stationary distribution and $\hat{x}(P) = (\hat{x}_1(P), ..., \hat{x}_n(P)).$

At this stationary distribution, the local long-term growth rate of species i in patch ℓ equals the difference between its average local per capita growth rate and one-half of the environmental variance experienced in patch ℓ :

$$r_i^{\ell}(\hat{x}, P) = \mu_i^{\ell}(P) - \frac{\sigma_i^{\ell\ell}}{2}, \tag{4}$$

where

$$\mu_i^{\ell}(P) = \sum_{j=1}^n a_{ij}^{\ell} \hat{x}_j(P) + b_i^{\ell}.$$

This local long-term growth rate describes the per capita growth of a population averaged across the fluctuations in species' densities and environmental conditions. As the per capita impacts of the environmental fluctuations on the per capita growth rates are density independent, the reduction $\sigma_i^{t\ell}/2$ in the local long-term growth rates are also density independent.

This local long-term growth rate characterizes the rate of growth for a subpopulation of species i permanently restricted to patch ℓ . If this local long-term growth rate is negative, such a subpopulation of such individuals would exponentially decline to extinction. Whenever this

occurs, patch ℓ is a long-term sink for species i. When the local long-term growth rate is negative because of the environmental fluctuations (i.e., $r_i^{\ell} < 0$ despite $\mu_i^{\ell} > 0$), growth rates in these patches fluctuate between positive and negative values over shorter timescales. Hence, we call these long-term sinks "stochastic sinks." Alternatively, if this local long-term growth rate is positive, then this patch is a long-term source patch for species i. As we discuss in the results section, all patches may be sink patches for species i despite species i persisting.

At the global scale, the global long-term growth rate of any of the coexisting species must equal zero, as their average densities in the long-term are not changing. As this global long-term growth rate is given by the difference between the mean growth rate $M_i(P)$ and one-half of the global environmental variance $V_i(P)$ experienced by species i, we have

$$M_i(P) - \frac{1}{2}V_i(P) = 0, \quad i = 1, 2, ..., n,$$
 (5)

where

$$M_i(P) = \sum_{\ell=1}^k p_i^\ell \mu_i^\ell$$
 and $V_i(P) = \sum_{\ell,m} p_i^\ell p_i^m \sigma_i^{\ell,m}$.

Importantly, equation (5) is a system of linear equations that allows one to easily solve for the mean species densities $\hat{x}_i(P)$. See section S1 on the supplemental PDF for a proof of equation (5).

Coevolutionarily Stable Strategies. To define a coESS P of patch selection, we consider a resident community of coexisting species playing patch selection strategy P. For one of these species—say, species i'—a mutation arises leading to patch selection strategy $\vec{q} = (q^1, ..., q^k) \neq \vec{p}_i'$. If y is the global population density of the mutant and x_i' is the density of the nonmutant individuals of species i', then the resident-mutant community dynamics become

$$dx_{i} = x_{i} \sum_{\ell=1}^{k} p_{i}^{\ell} \left(\left(\sum_{j=1}^{n} a_{ij}^{\ell} p_{j}^{\ell} x_{j} + a_{ii}^{\ell} q^{\ell} y + b_{i}^{\ell} \right) dt + dE_{i}^{\ell} \right),$$

$$i = 1, 2, ..., n,$$

$$dy = y \sum_{\ell=1}^{k} q^{\ell} \left(\left(\sum_{j=1}^{n} a_{ij}^{\ell} p_{j}^{\ell} x_{j} + a_{i'i}^{\ell} q^{\ell} y + b_{i'}^{\ell} \right) dt + dE_{i'}^{\ell} \right).$$
(6)

Importantly, the mutant y only differs from the resident in its patch selection strategy \vec{q} . It has the same interaction coefficients a_{ij} and intrinsic rates of growth b_i as the resident x_i and experiences the same environmental stochasticity E_i^p as the resident x_i .

When mutant population density is low and the resident community coexist about a stationary distribution, the long-term growth rate, also known as the invasion growth rate, of the mutant population against the resident community is

$$\mathcal{I}_{i'}(P, \vec{q}) = \sum_{\ell=1}^{k} q^{\ell} \mu_{i'}^{\ell}(P) - \frac{1}{2} V_{i'}(\vec{q}). \tag{7}$$

If $\mathcal{I}_{i'}(P, \vec{q}) < 0$, then the mutant is very likely to become asymptotically extinct. In particular, the probability of the mutant becoming asymptotically extinct is arbitrarily close to 1 when its initial density is arbitrarily small (see the supplemental PDF, sec. S2).

We define P to be a coESS if for every species i, mutants playing a different strategy $\vec{q} \neq \vec{p}_i$ cannot invade the community (i.e., $\mathcal{I}_i(P, \vec{q}) < 0$; see the supplemental PDF, sec. S2). When the environmental fluctuations are not perfectly correlated between any pair of patches (i.e., the covariance matrices \sum_i are nondegenerate), we show in section S2 of the supplemental PDF that it suffices to check the weaker condition: $\mathcal{I}_i(P, \vec{q}) \leq 0$ for all i and $\vec{q} \neq \vec{p}_i$. This condition is easier to verify algebraically.

Analytical and Numerical Approaches for the coESS. Our Nash equilibrium condition for the coESS and the explicit analytical expressions for the invasion growth rates can be used in conjunction with the method of Lagrange multipliers to identify a necessary condition for the coESS. This result and its implications are presented in the results section.

To solve for the coESS numerically, we describe in section S3 of the supplemental PDF an evolutionary dynamic on the strategy space for all of the species in which small mutations occurring at a rate ν randomly shuffle the "infinitesimal" weights of our species' patch selection strategy. This results in a replicator-type equation,

$$\frac{dp_i^{\ell}}{dt} = \nu p_i^{\ell} \left(\frac{\partial \mathcal{I}_i}{\partial q_i^{\ell}} (P, \vec{p}_i) - \sum_{m} p_i^{m} \frac{\partial \mathcal{I}_i}{\partial q_i^{m}} (P, \vec{p}_i) \right), \quad (8)$$

where $(\partial \mathcal{I}_i/\partial q_i^\ell)(P,\vec{p}_i)$ denotes $(\partial \mathcal{I}_i/\partial q_i^\ell)(P,\vec{q})$ evaluated at $\vec{q}=\vec{p}_i$. Equation (8) is a multispecies version of the trait dynamics derived in Schreiber (2012). In section S3 of the supplemental PDF, we show that equilibria of equation (8) satisfy the derivative conditions for a coESS. We simulate equation (8) using the deSolve package from R (Soetaert et al. 2010). In all cases, these simulations converged to an equilibrium that satisfied the necessary conditions for a coESS. We note that even though the right-hand side of equation (8) for a fixed value of P corresponds to the gradient of the function $h(\vec{q}) = \mathcal{I}_i(P,\vec{q})$ with respect to the Shahshahani metric (Hofbauer and Sigmund 1998), this is not a gradient ascent method, as a coESS (like an ESS) need not maximize the function \mathcal{I}_i . The coESS

command in the R code (Schreiber 2023) implements this numerical method.

Results

We begin by presenting a characterization of the coESS and its implications for any number of species. This characterization provides answers to the following questions: What, if any, quantities are equalized across the occupied patches? When is there evolution of sink populations? When and how do occupying multiple patches buffer against temporal variability? After answering these questions, we focus on models of antagonistic interactions.

Characterization of the coESS and General Implications

The coESS Balances Local Contributions to the Global Long-Term Growth Rates. Our analysis reveals that for species playing the coESS, there is a demographic quantity associated with each patch that is equalized across all occupied patches. This demographic quantity corresponds to the difference between the local contributions to the mean and variances of the global long-term growth rate. Consequently, occupied patches with higher contributions to the mean also experience higher contributions to the variance. Intuitively, if there were a patch that contributed relatively more to the mean than the variance, then a mutant subpopulation allocating more individuals to this patch would simultaneously increase their mean rate of growth and decrease the variance in their growth rate. Thus, this mutant would have a higher global long-term growth rate than the residents and could invade.

To describe these local contributions precisely, recall that the global long-term growth rate of species i equals the difference between the global mean $M_i(P)$ and one-half of the global variance $V_i(\vec{p})$. As the mean of the global growth rate is the weighted combination of the means of the local growth rates (i.e., $M_i = \sum_{\ell} p_i^{\ell} \mu_i^{\ell}$), we call μ_i^{ℓ} the contribution of patch ℓ to M_i . The variance of the global growth rate equals the sum of the environmental covariances $\sigma_i^{\ell m}$ weighted by the probability that two randomly chosen individuals are in patches ℓ and m:

$$V_i(\vec{p}_i) = \sum_{\ell,m} p_i^m p_i^{\ell} \sigma_i^{\ell m}.$$

The variance V_i can be expressed as a weighted sum of the covariances between the environmental fluctuations experienced in patch ℓ by species i and the environmental fluctuations experienced by a randomly chosen individual of species i. This covariance for species i in patch ℓ equals

$$\sigma_i^{\ell}(\vec{p}_i) = \sum_m p_i^m \sigma_i^{\ell m}.$$

The global variance V_i equals the weighted sum of these covariances

$$V_i(\vec{p}_i) = \sum_{\ell} p_i^{\ell} \sigma_i^{\ell}(\vec{p}_i),$$

and therefore we call σ_i^ℓ the contribution of patch ℓ to V_i . For each species playing the coESS, we show in section S4 of the supplemental PDF that the difference between the local contributions, μ_i^ℓ and σ_i^ℓ , to the mean global growth rate M_i and the global variance V_i are equal in all occupied patches. Moreover, the common value of these differences equals the difference between the global growth rate M_i and the global variance V_i . Mathematically,

$$\mu_i^{\ell} - \sigma_i^{\ell}(\vec{p}_i) = M_i(P) - V_i(\vec{p}_i)$$

in patches ℓ occupied by species i and

$$\mu_i^{\ell} - \sigma_i^{\ell}(\vec{p}_i) \le M_i(P) - V_i(\vec{p}_i) \tag{9}$$

in patches ℓ not occupied by species i.

For the unoccupied patches, inequality (9) is strict whenever \sum_i is nondegenerate; for example, the environmental fluctuations for species i are positive in all patches, and no pair of patches has perfectly correlated environmental fluctuations.

Using the coESS condition (9), we can answer three questions about patch selection: When does the coESS correspond to an ideal free distribution? When do species evolve to use multiple habitat patches? When is there selection for spatial buffering?

Ideal Free Distributions Are the Exception, Not the Norm. Consistent with classical ideal free distribution theory, when there are no environmental fluctuations ($\sigma_i^{\ell m} = 0$ for all ℓ , m), the coESS condition (9) implies that the local long-term growth rates are equal in all occupied patches (i.e., $\mu_i^{\ell} = 0$ in all occupied patches, as $V_i = \sigma_i^{\ell} =$ $M_i = 0$) and lower in unoccupied patches (i.e., $\mu_i^{\ell} \leq 0$). In fluctuating environments, however, the local long-term growth rates in general need not be equal in all patches. This occurs as the nonlocal quantities $\mu_i^{\ell} - \sigma_i^{\ell}$ in coESS conditions (9) typically do not equal the local long-term growth rates $\mu_i^{\ell} - \sigma_i^{\ell\ell}/2$. One important exception occurs when the environmental fluctuations are perfectly correlated and have the same magnitude across all patches (i.e., $\sigma_i^{\ell m}$ are equal for all ℓ , m). In this case, the covariances σ_i^{ℓ} , the local variances $\sigma_i^{\ell\ell}$, and the global variance V_i are all equal. Consequently, the coESS condition (9) implies that the local long-term growth rates $\mu_i^{\ell} - \sigma_i^{\ell\ell}/2$ equal zero in all of the occupied patches. Figure 3*B*–3*D* illustrates how this ideal free distribution breaks down with reduced spatial correlations in a predator-prey system.

Patches Acting as Environmental Buffers Are Long-Term Deterministic Sinks. A patch buffers a species against environmental fluctuations when the fluctuations within the patch are negatively correlated with the average fluctuations experienced by the species (i.e., σ_i^ℓ is negative). The coESS condition (9) provides some insights into when such buffering occurs. As the global long-term growth rate $M_i - V_i/2$ equals zero, the difference $M_i - V_i$ equals the negative quantity $-V_i/2$. Hence, in patches acting as buffers, the local mean growth rate is negative, and consequently these patches are long-term deterministic sinks (i.e., $\mu_i^\ell - \sigma_i^\ell = -V_i/2$ and $\sigma_i^\ell < 0$ implies that $\mu_i^\ell < 0$).

Whenever Multiple Patches Are Occupied, All Are Long-Term Sinks. Provided there is some spatial asynchrony in the environmental fluctuations experienced by species i (i.e., \sum_i is nondegenerate), the patch selection strategy of species i at the coESS exhibits a fundamental dichotomy (proposition S4.1 in sec. S4 of the supplemental PDF): species i either occupies only one patch or occupies multiple patches, and the local long-term growth rates are negative in these occupied patches. Thus, if species i occupies multiple patches at the coESS, then all of its populations are long-term sink populations despite it persisting globally. This occurs because species playing the coESS exhibit a form of spatial bet hedging that results in the global stochastic growth rate being greater, specifically zero, than the local stochastic growth rates (see the discussion section).

Evolution for occupying a single patch in the landscape occurs only when the other patches are long-term sinks. Moreover, these sinks must lead to sufficiently negative long-term growth rates or exhibit similar environmental fluctuations as the occupied patch. More precisely, our coESS condition (9) (proposition S4.2 in sec. S4 of the supplemental PDF) implies that only patch ℓ is occupied if

$$\mu_i^m - \frac{1}{2}\sigma_i^{mm} < -\frac{1}{2}\overbrace{(\sigma_i^{\ell\ell} - 2\sigma_i^{\ell m} + \sigma_i^{mm})}^{\text{Var}[E_i^r(1) - E_i^m(1)]}$$
for all other patches $m \neq \ell$.

To better understand inequality (10), consider the case where the environmental fluctuations for species i in all patches have variance σ^2 and spatial correlation ρ (i.e., $\sigma_i^{\ell\ell} = \sigma^2$ for all ℓ and $\sigma_i^{\ell m} = \rho \sigma^2$ for $\ell \neq m$). Then, condition (10) requires that the long-term growth rates in the unoccupied patches m are less than $-\sigma^2(1-\rho)$. Hence, selection for only occupying patch ℓ is greatest when the environmental fluctuations across patches are strongly positively correlated ($\rho \approx 1$).

Applications to Antagonistic Interactions

Antagonistic interactions, such as the interactions between predators and their prey or between competing species, can result in reciprocal selection pressures. Here, we investigate how this reciprocal evolution can either lessen the antagonism by selecting for divergent choices in patch use or enhance the antagonism by selecting for convergent choices in patch use.

Predator-Prey Coevolution

A General Model. We begin with a predator-prey system where x_1 and x_2 are the global densities of the prey and predator, respectively. The intrinsic per capita growth rate of the prey in patch ℓ is r^{ℓ} . The predator is a specialist on the prey with attack rates, conversion efficiencies, and per capita death rates in all patches equal a, c, and d, respectively. As the predator is a specialist, it cannot persist in the absence of the prey species. To ensure stability of the predator-prey dynamics, we assume that both species experience weak intraspecific competition with strength $\alpha \gtrsim 0$. Under these assumptions, the Lotka-Volterra model takes on the form

$$dx_{1} = x_{1} \left(\sum_{\ell} p_{1}^{\ell} ((r^{\ell} - \alpha p_{1}^{\ell} x_{1} - a p_{2}^{\ell} x_{2}) dt + p_{1}^{\ell} dE_{1}^{\ell}) \right),$$

$$dx_{2} = x_{2} \left(\sum_{\ell} p_{2}^{\ell} ((cap_{1}^{\ell} x_{1} - \alpha p_{2}^{\ell} x_{2} - d) dt + p_{2}^{\ell} dE_{2}^{\ell}) \right).$$
(11)

In section S5 of the supplemental PDF, we derive criteria that characterize when the species coexist globally and find explicit expressions for the mean densities of the species at stationarity and the invasion growth rates $\mathcal{I}_i(\vec{p}, \vec{q})$. Here, we focus on two cases: a two-patch sink-source system and an environmental gradient for the prey.

A Two-Patch Source-Sink System. Consider a landscape where the prey has a source habitat (patch 1 with r^1 = $r_{\text{source}} > 0$) and a sink habitat (patch 2 with $r^2 = -r_{\text{sink}}$). The sink habitat is low quality but exhibits minimal environmental fluctuations ($\sigma_1^{22} = \sigma_2^{22} = 0$), while the predator and prey experience environmental fluctuations in the source habitat with variances v_{prey} and v_{pred} respectively.

First, we study the effects of environmental stochasticity on the species individually and then collectively. If only the prey experiences environmental stochasticity in the source patch ($v_{prey} > 0$ and $v_{pred} = 0$), then the coESS has neither species occupying the sink patch for low values of v_{prey} , the prey occupying both patches at intermediate values of v_{prey} , both species occupying both patches at higher values of v_{prey} , the predator no longer

occupying the source patch at even higher values of v_{prey} , and, finally, extinction of both species when v_{prey} is too high (fig. 1A, 1B).

More specifically, when the environmental variance in the source patch is sufficiently low relative to the rate of loss in the sink patch ($v_{\text{prey}} < 2r_{\text{sink}}$), inequality (10) implies that the prey occupies only the source patch. As the coESS condition (9) requires that the growth rate of the predator is equal to zero in any patch it occupies, the predator also occupies only the source patch. When the environmental variance in the source patch exceeds $2r_{\text{sink}}$ but lies below $8r_{\text{sink}}$, the coESS conditions (9) imply that the fraction of prey living in the sink patch equals

$$f_{\text{prey}} = 1 - \sqrt{\frac{2r_{\text{sink}}}{\nu_{\text{prey}}}}.$$
 (12)

Equation (12) implies that the fraction of prey in the sink patch increases with the environmental variance v_{prey} in the source patch (fig. 1A). As the predator regulates the mean prey density in the source patch to the predator's break-even point d/ca, selection for prey using the sink patch results in higher mean prey densities (fig. 1B; supplemental PDF, sec. S5). These trends continue with increasing variation in the environmental fluctuations until 50% of the prey make use of the sink patch.

When the environmental stochasticity in the source patch selects for the prey being equally distributed between the patches (i.e., $8r_{\text{sink}} \le v_{\text{prey}} \le 8r_{\text{source}}/3$ and $3r_{\text{sink}} \leq r_{\text{source}}$; supplemental PDF, sec. S5), the predator evolves to use both patches. The fraction of predators using the sink patch equals

$$f_{\text{pred}} = \frac{\nu_{\text{prey}} - 8r_{\text{sink}}}{8r_{\text{source}} - 8r_{\text{sink}} - 2\nu_{\text{prey}}}.$$
 (13)

Equation (13) implies that the fraction f_{pred} of predators in the sink patch increases with the environmental stochasticity v_{prey} experienced by the prey. As the predator does not directly experience environmental stochasticity, it regulates the prey density, on average, to its break-even point in both patches. Hence, for this range of environmental variation, the mean global density of the prey is twice as high as when both species reside only in the source patch (fig. 1B). In contrast, the predator's mean global density decreases with increasing variation in the environmental fluctuations (fig. 1B).

When the variation in the environmental fluctuations are sufficiently large $(v_{\text{prey}} \ge (8/3)r_{\text{sink}})$ but not so large as to cause extinction, the predator evolves to use only the sink patch (i.e., $f_{pred} = 1$), while the prey continues to use both

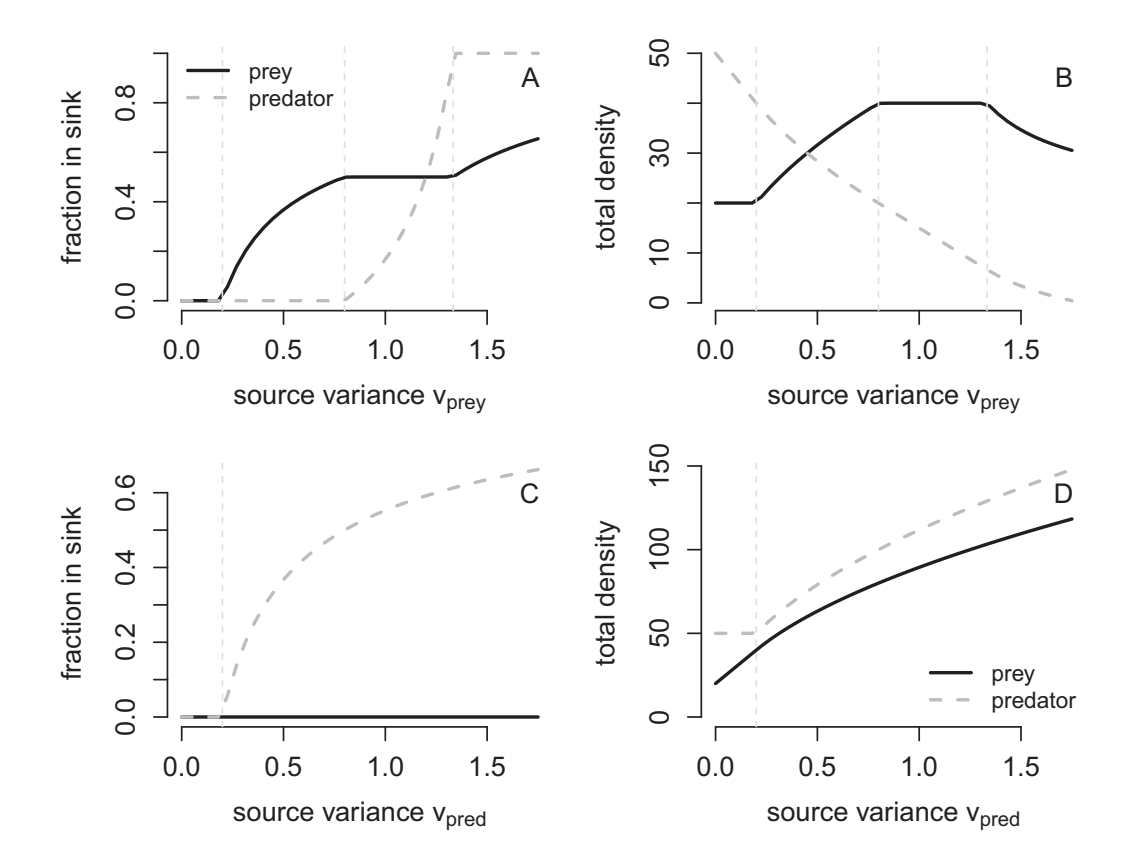


Figure 1: Predator-prey interactions and environmental fluctuations select for enemy-free patches and victimless patches in a source-sink system. In A and B, the prey experience environmental fluctuations in the source patch with variance v_{prey} . In C and D, the predator experiences environmental fluctuations in the source patch with variance v_{pred} . Solid and dashed thick lines correspond to numerically estimated solutions by simulating equation (8) for 2,000 time steps. Dashed thin vertical lines correspond to the analytic conditions for changes in patch use presented in the main text. Parameters: $r_{\text{source}} = 0.5$, $r_{\text{sink}} = 0.1$, d = 0.1, a = 0.01, c = 0.5, intraspecific competition coefficient of $\alpha = 0.000001$ for both species.

patches. When this occurs, the fraction of prey making use of the sink patch equals (supplemental PDF, sec. S5)

$$f_{\text{prey}} = \sqrt{1 - \frac{2r_{\text{sink}}}{\nu_{\text{prey}}}}.$$
 (14)

Equation (14) implies that the fraction of prey in the sink patch continues to increase with increasing variation of the environmental fluctuations. In contrast, the mean global prey density decreases with the environmental variance (fig. 1*B*; supplemental PDF, sec. S5). When the environmental fluctuations are sufficiently strong, $v_{\rm prey} \ge (1/2)((r_{\rm sink} + r_{\rm source})^2/r_{\rm sink})$, both species become extinct (not shown in fig. 1).

When only the predator experiences environmental stochasticity in the source patch ($\nu_{\rm pred} > 0$ and $\nu_{\rm prey} = 0$), the coESS condition (9) implies that the prey's growth rate is zero in all occupied patches. Consequently, prey playing the coESS occupy only the source patch. Despite a victim-

less sink patch, the predator evolves to occupy the sink patch whenever the environmental variance in the source patch is sufficiently great (i.e., $v_{\rm pred} > 2d$). Under these circumstances, the fraction of predators using the sink patch equals

$$f_{\text{pred}} = 1 - \sqrt{\frac{2d}{\nu_{\text{pred}}}}.$$
 (15)

Equation (15) implies that greater environmental variation in the source patch selects for greater use of the sink patch (fig. 1*C*). When the predator makes use of the sink patch, the mean global density of both species playing the coESS increases with the environmental variance in the source patch (fig. 1*D*; supplemental PDF, sec. S5). Intuitively, as the environmental fluctuations increase, the predator has a higher break-even prey density in the source patch that determines the mean prey density. These higher prey densities in turn lead to higher mean predator densities.

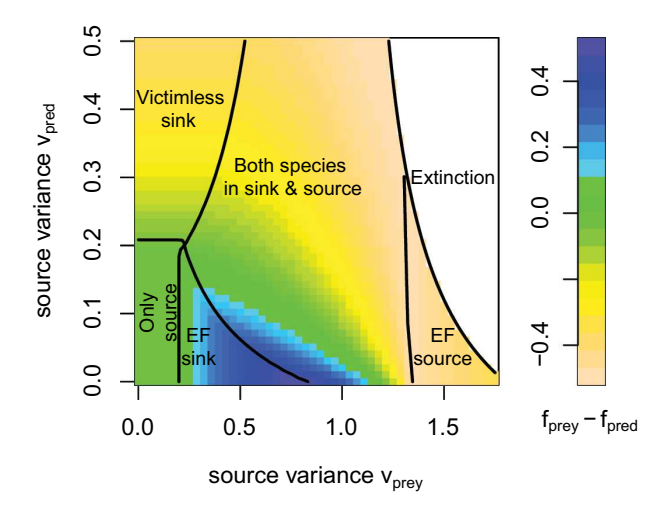


Figure 2: Simultaneous environmental fluctuations for predator and prey select for enemy-free (EF) patches, victimless sinks, and predator-prey interactions in sink patches. The white region corresponds to environmental variation that leads to the extinction of both species. Colors represent the difference in the fraction of prey and predators in the sink patch. Parameters are as in figure 1.

Figure 2 illustrates the effects of simultaneous environmental variation on both species on the coESS. Consistent with the predictions from varying environmental stochasticity for only one species, high environmental variation for the predator selects for victimless sinks when variation for the prey is sufficiently low and selects for both species using both patches when this variation is sufficiently high. In contrast, low environmental variation for the predator selects for enemy-free sinks, both species using the sink patch, and enemy-free sources with increasing levels of environmental variation for the prey.

Patch Selection along an Environmental Gradient. Using our numerical algorithm, we examined patch selection along a gradient of environmental fluctuations. Along this gradient, the environmental variance experienced by both species varies in a Gaussian manner (fig. 3A). In the center of the landscape where environmental fluctuations are strongest, the patches are long-term stochastic sinks (patches between dashed vertical lines in fig. 3). When the environmental fluctuations are spatially uncorrelated, all patches

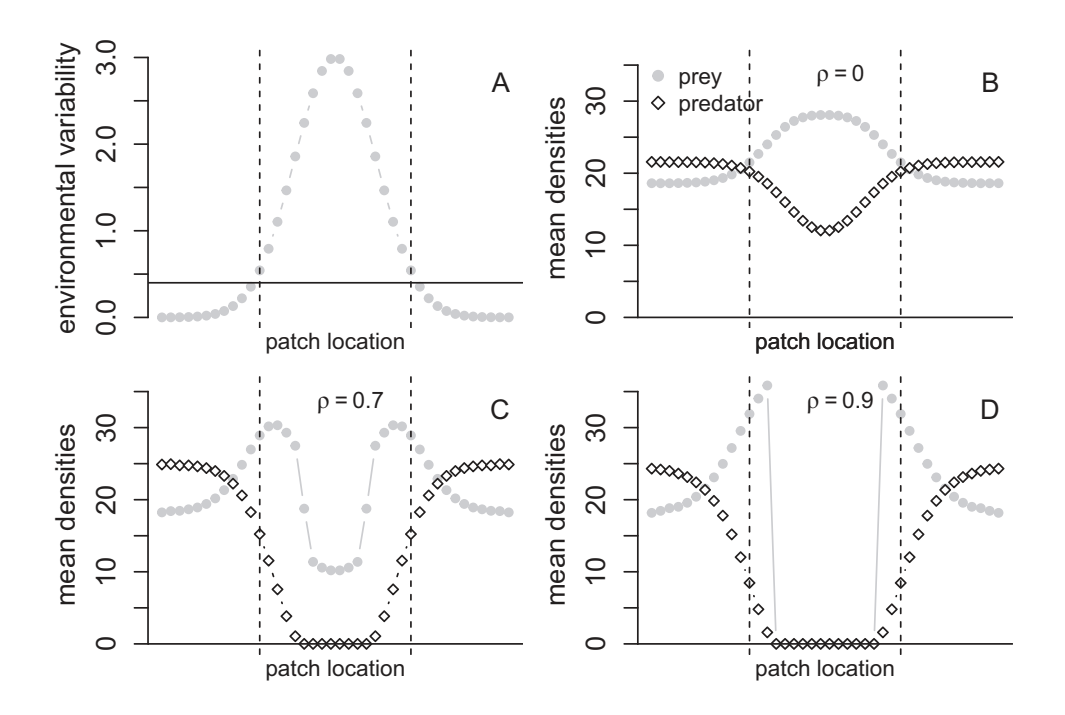


Figure 3: Spatial correlations in environmental fluctuations exorcise predators and their prey from sink patches along a spatial gradient. Both species experience environmental fluctuations whose strength decay from a central location in the landscape (A). The horizontal line in A corresponds to twice the prey's intrinsic rate of growth (2r'). Patches between the vertical dashed lines are long-term sources for the prey. Patches outside the vertical dashed lines are long-term stochastic sinks for the prey. The spatial correlation $\rho^{|\ell-m|}$ between two patches ℓ and m decays with distance, where ρ is the spatial correlation between two neighboring patches (i.e., $|\ell - m| = 1$). The mean densities of the predator (white diamonds) and prey (gray circles) are plotted for the coevolutionarily stable strategy at three levels of correlation ρ (B-D). Parameters: n=2 species; k=40 patches; $r^{\ell}=0.1$; $a^{\ell} = 0.01; c^{\ell} = 0.5; d^{\ell} = 0.1 \text{ for all } \ell; \sigma_i^{\ell m} = \rho^{|\ell-m|} \sqrt{\nu^{\ell} \nu^{m}}, \text{ where } \nu^{\ell} = 3 \exp(-(z^{\ell})^2) \text{ for } z^{\ell} = 6/\ell - 3 \text{ and } 1 \le \ell \le 40; \alpha = 0.00001.$

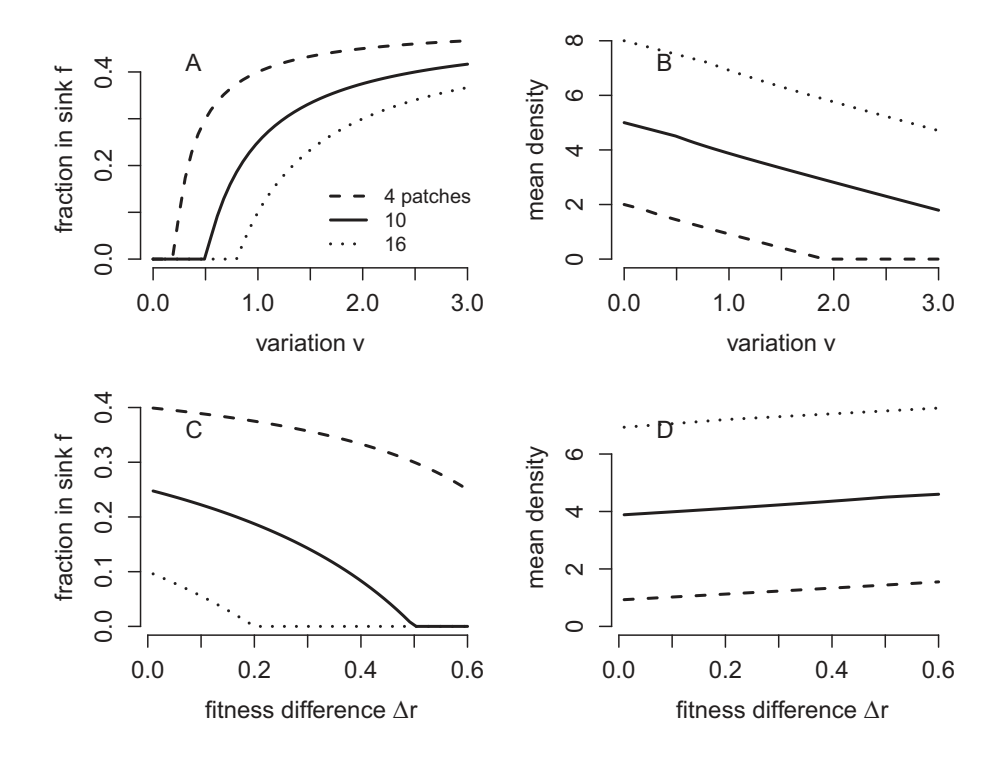


Figure 4: Smaller fitness differences $(\Delta r = \bar{r} - \underline{r})$, greater environmental variation (v), and fewer number of patches (k) help exorcise the ghost of competition past. The fraction of competitors (f) using the patches in which they are the inferior competitor is plotted in A and C. Exorcism of the ghost of competition past occurs when f > 0. The mean global density of each competitor is plotted in B and D. Parameters: $\bar{r} = 1$ in all panels, $\underline{r} = 0.9$ in A and B, $\underline{r} = 1 - \Delta r$ and v = 1 in C and D.

are occupied by both species, but the species exhibit contrary choices: the two species exhibit negatively correlated patch selection strategies. (fig. 3*B*). Spatial correlations in the environmental fluctuations selects for both species exhibiting reduced preferences and lower densities in the most central patches (fig. 3*C*, 3*D*). When these spatial correlations are sufficiently strong, neither species occupies the central patches, consistent with the general prediction of approaching an ideal free distribution (fig. 3*D*). For intermediate spatial correlations, only the predator avoids the central patches, creating enemy-free sinks (fig. 3*C*).

Exorcising the Ghost of Competition Past

A General Model. To understand how spatial-temporal heterogeneity selects for spatial distributions of competing species, we examine a model of two species competing in k patches. This analysis provides insights into when competitors evolve to never occupy the same patches (i.e., the ghost of competition past; Lawlor and Maynard Smith 1976; Connell 1980) or evolve to co-occur within patches (i.e., exorcising the ghost). For competitor i in the model, its intrinsic rate of growth in patch ℓ is r_i^ℓ . The average per capita growth rates decrease linearly with the local den-

sity of both competitors. Namely, the average per capita growth rate of species i in patch ℓ equals $r_i^{\ell} - \sum_j p_j^{\ell} x_j$. Thus, the global dynamics are

$$dx_i = \sum_{\ell} p_i^{\ell} x_i \left(\left(r_i^{\ell} - \sum_j p_j^{\ell} x_j \right) dt + dE_i^{\ell} \right). \tag{16}$$

These competitors, in general, cannot coexist locally: the species with the larger intrinsic stochastic growth rate $r_i^\ell - \sigma_i^{\ell\ell}/2$ in patch ℓ excludes the other species in the absence of immigration. Global coexistence, however, is possible in a multipatch landscape. In section S6 of the supplemental PDF, we derive criteria that characterize when the species coexist globally, the mean equilibrium densities of the species at the associated stationary distribution, and explicit expressions for the invasion rates of mutant strategies against resident strategies. Here, we focus on two cases: two species in a spatially symmetric landscape and three species living along an environmental gradient.

Competition along a Symmetric Landscape. Imagine a symmetric landscape with an even number of patches where each species has the competitive advantage in half of the landscape. The average per capita growth rate for species i equals \bar{r} in the patches where it is competitively

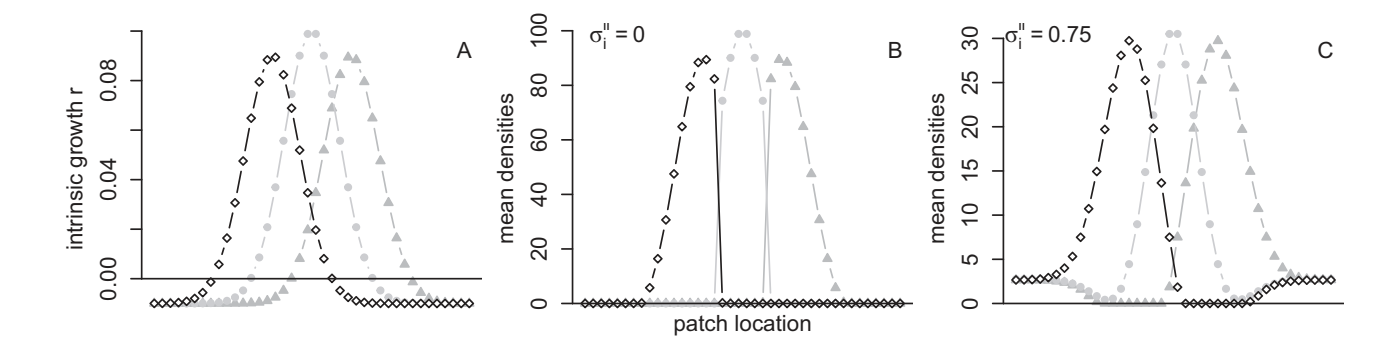


Figure 5: Coevolution of patch selection for three competing species can create complex spatial distributions along an environmental gradient. In *A*, the environmental variation in the average intrinsic rates of growth r_i^t is shown for all three species. In *B* and *C*, the mean densities of all three species playing the coevolutionarily stable strategy in the absence (*B*) and presence (*C*) of environmental stochasticity are shown. Parameter values: n=3 species; k=40 patches; $r_i^t=0.1 \exp(-(z^\ell-1)^2)-0.01$; $r_i^t=0.1 \exp(-(z^\ell)^2)-0.01$; $r_i^t=0.1 \exp(-(z^\ell+1)^2)-0.01$ for $z^t=8/\ell-4$ and $1\leq \ell \leq 40$; $a_{ij}^t=-0.001$ for all i,j,ℓ ; $\sum_i=\sigma^2 \operatorname{Id}$ with $\sigma^2=0$ in *B* and $\sigma^2=0.75$ in *C*.

superior and equals $\underline{r} < \overline{r}$ in the patches where it is competitively inferior. Each species experiences spatially uncorrelated environmental fluctuations with local variance ν . Our analysis reveals that there is critical level of environmental variance below which the species never occupy the same patch and above which this ghost of competition past is exorcised. The critical level of variance depends both on the number of patches in the landscape and on the fitness difference of the competitors.

To see why these conclusions hold, the symmetry of the landscape implies that any coESS for the competing species satisfies that a fraction f of individuals use the patches where they have competitive disadvantage (sink patches), and the complementary fraction 1-f use the patches where they have a competitive advantage (source patches). At the coESS (for details, see the supplemental PDF, sec. S6), each species uses only the source patches (i.e., f=0) if

$$\Delta r \coloneqq \bar{r} - \underline{r} > \frac{2\nu}{k}.\tag{17}$$

Equation (17) implies that if the environmental variance ν is too low relative to the number of patches or if the fitness difference Δr is too large, then evolution selects for the competitors to be spatially segregated, that is, the ghost of competition past prevails (left- and right-hand sides of fig. 4A, 4C, respectively).

When environmental fluctuations are sufficiently large (i.e., ineq. [17] is reversed), evolution selects for both species to use both patch types with

$$f =$$
the fraction in sink patches $= \frac{1}{2} - \frac{k\Delta r}{4\nu};$ (18)

that is, the ghost of competition past is partially exorcised. Equation (18) implies that the majority of individuals (i.e., 1-f > 1/2) occupy their source patches. However, for smaller fitness differences Δr or higher levels of environmental variation ν , evolution selects for both species to be spread more equally across the patches (i.e., right- and left-hand sides of fig. 4A, 4C, respectively).

Whether sink patches are occupied or not, the mean global density of each competitor equals

$$\frac{k}{2}(\bar{r} - f\Delta r) - \frac{\nu}{2}(f^2 + (1 - f)^2). \tag{19}$$

When the competitors are spatially segregated (i.e., f=0), the equilibrium density $(k\bar{r}/2-\nu/2)$ is a decreasing linear function of the environmental variation (fig. 4*B*). Selection for the use of both patch types (i.e., f>0) results in a nonlinear, accelerated, negative response of mean density to increasing environmental variation.

Three Species Competition along an Environmental Gradient. Using our numerical algorithm, we also explored the coevolution of patch selection for three competing species along an environmental gradient (fig. 5). Along this gradient, the species differed in their intrinsic rates of growth and experienced the same amount of environmental stochasticity (fig. 5A). In the absence of environmental fluctuations, the coESS corresponds to an ideal free distribution resulting in each species occupying only the patches in which their intrinsic stochastic growth rates are positive and in which they are competitively superior (fig. 5B). Notably, the species are spatially segregated and occupy no sink patches. In the presence of environmental fluctuations, each patch is occupied by at least two species—the ghost of competition past is partially exorcised (fig. 5C). Moreover, at the center and edges of the landscape, all three species co-occur.

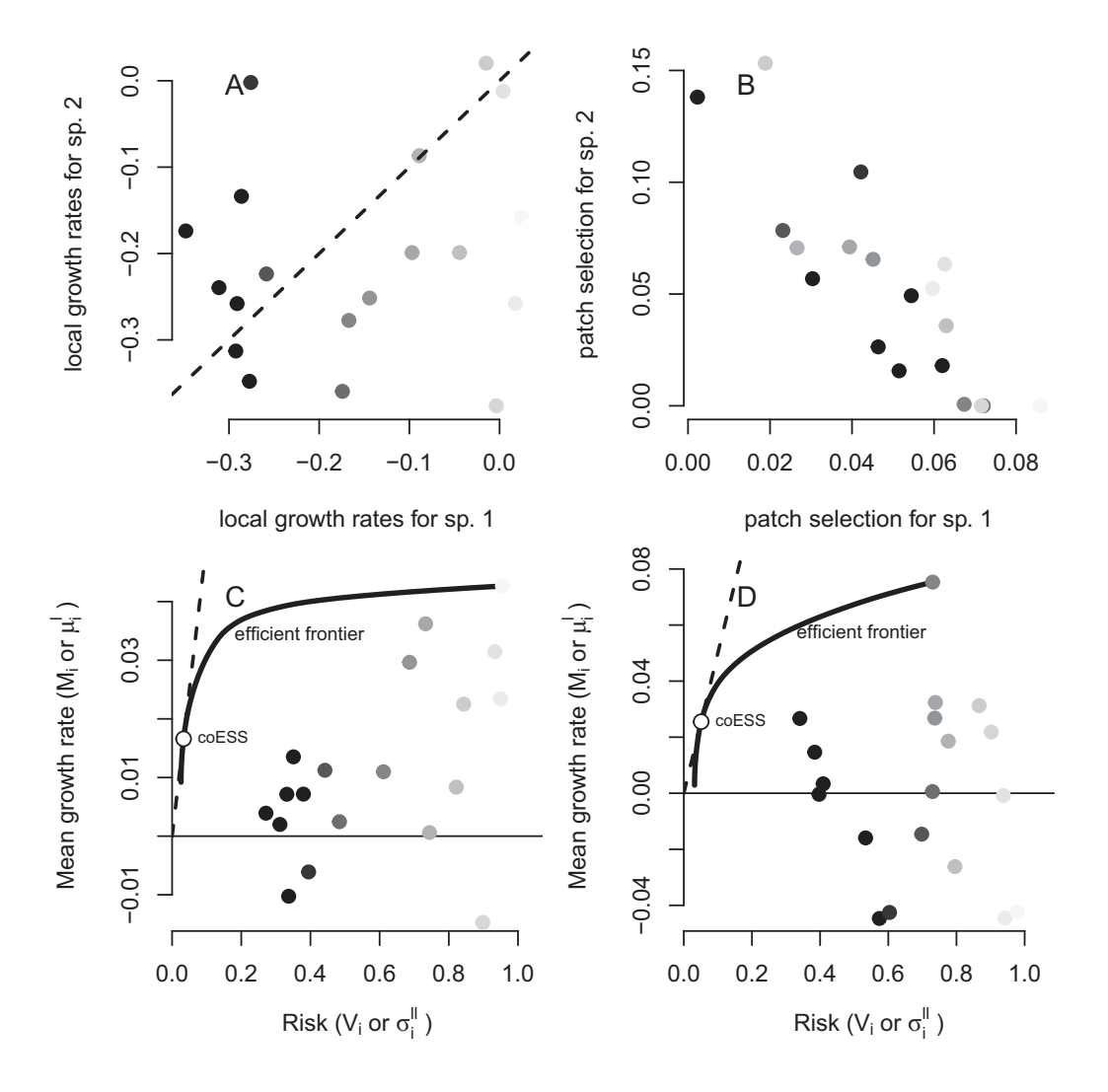


Figure 6: The coevolutionarily stable strategy (coESS) of patch selection through the lens of modern portfolio theory (MPT). The comparison considers two competing species in a 20-patch landscape with differing local long-term growth rates (*A*). These local long-term growth rates determine local competitive superiority. The coESS for patch selection (*B*) exhibits a negative correlation between the competitors. At the coESS, the local mean growth rates and local variances are plotted in the mean-variance plane for each of the species (*C*, *D*). The efficient frontier (see the main text) is plotted as a solid line, the global means and variances associated with the coESS are plotted as a white circle, and the dashed line is where the global stochastic growth rate equals zero.

At the edges, the co-occurring species are long-term deterministic sink populations.

Discussion

Unlike classical ideal free theory that predicts selection against sink populations under equilibrium conditions (Fretwell and Lucas 1969; Křivan et al. 2008), we find that coevolution in fluctuating environments often selects for metacommunities consisting entirely of long-term sink populations. The difference stems from what selection equalizes across the occupied landscape under equilibrium versus non-equilibrium conditions. Under equilibrium conditions, the

per capita growth rates of all populations are equal to zero in occupied patches and negative in unoccupied patches. Hence, there are no sink populations. In landscapes with environmental stochasticity, coevolution of patch selection no longer equalizes the mean per capita growth rates in occupied patches. Instead, the differences between the means of the local per capita growth rates and the covariance between the local and global fluctuations are equalized. Whenever there is evolution for occupying multiple patches, equalizing these differences sacrifices higher mean growth rates for lower variances of these growth rates and results in negative long-term growth rates in all occupied patches. This spatial bet hedging can be understood through the

lens of the modern portfolio theory (MPT) of economics (Markowitz 1952, 1991; Rubinstein 2002; Markowitz 2010), as we discuss below. The resulting sink populations may be conditional due to the presence of antagonistic interactions or unconditional. In particular, environmental stochasticity coupled with predator-prey interactions can select for enemy-free sinks and victimless sinks (Jeffries and Lawton 1984). Alternatively, environmental stochasticity coupled with competitive interactions can select for a conditional sink population by partially exorcising the ghost of competition past (Lawlor and Maynard Smith 1976; Connell 1980; Schmidt et al. 2000).

Relation to MPT

MPT (Markowitz 1952, 1991, 2010) is a Nobel Prizewinning framework for assembling a portfolio of financial investments. In this framework, each investment has a mean return and some level of risk characterized by the variance in the return. In our context, investments correspond to patches, mean returns of investments correspond to mean local growth rates μ_i^{ℓ} , and risks correspond the local environmental variances $\sigma_i^{\ell\ell}$ (fig. 6A). A patch selection strategy (fig. 6B) \vec{p}_i corresponds to a portfolio of investments (i.e., a fixed allocation of assets across the investments). The global mean growth rate M_i and the global environmental variance V_i of a patch selection strategy corresponds to the mean return and variance of a portfolio of investments, respectively. MPT assumes that investors prefer portfolios with high mean returns and avoid those with high risk. As investments with high mean returns often are high-risk investments, investments often exhibit a meanvariance trade-off (Zivot 2017). In our context, however, patches themselves need not exhibit a mean-variance trade-off; high-quality patches may consistently support high mean growth rates, and low-quality patches may be highly variable. Instead, the mean-variance trade-off stems from the long-term growth rate increasing with the mean but decreasing with the variance $(M_i - V_i/2)$ or $\mu_i^{\ell\ell} - \sigma_i^{\ell\ell}/2$), the cornerstone of bet-hedging theory in evolutionary biology (Cohen 1966; Stearns 2000; Childs et al. 2010). Markowitz (1952) showed that for a given level of risk *V*, there are portfolios maximizing the mean return M for that level of risk. These optimal portfolios can be solved for only using matrix algebra (Zivot 2017). The curve of means and variances determined by these portfolios is the efficient frontier (solid curves in fig. 6C, 6D). Markowitz (1952) showed that the efficient frontier also corresponds to the portfolios minimizing an investor's risk for a given mean return. In our context, the coESS patch selection strategy must be a point on the efficient frontier (white circles in fig. 6C, 6D). Indeed, if it was not, there would be an alternative patch selection strategy either providing lower risk for

the same mean return or providing a greater mean return for the same amount of risk. In either case, such a patch selection strategy would have a higher global long-term growth rate $M_i - V_i/2$ than residents playing the coESS contradicting the definition of a coESS. By lying on the efficient frontier, the coESS typically sacrifices a higher global mean growth rate for a lower global variance (all of the local mean growth rates are greater than the mean growth rate of the coESS in fig. 6C, 6D). Hence, the coESS typically is a bet-hedging strategy (Childs et al. 2010). The only exception occurs when the mean growth rates are equal in all occupied patches. Only then can the coESS reduce risk without reducing the mean. Furthermore, as the global long-term growth rate $M_i - V_i/2$ is zero, the coESS corresponds to the point on the efficient frontier that is tangent to the $M_i = V_i/2$ line (see the white circle and dashed lines in fig. 6C, 6D)—in economic terms, a tangent portfolio associated with a risk-free zero-return asset (Zivot 2017). Whenever multiple patches are occupied at the coESS, all of the points in the mean-variance plane corresponding to the individual patches (i.e., individual investments) lie below the efficient frontier and consequently have negative local long-term growth rates (see the shaded circles in fig. 6C, 6D). Hence, all patches are long-term sinks.

Ghosts of Past and Present Antagonisms

Patches free of antagonistic interactions may reflect habitat selection in response to past antagonisms within a patch or present antagonisms in other patches. Spatial heterogeneity can select for ghosts of competition past or enemy-free space by creating spatial mosaics of environmental conditions favoring one species over another (Lawlor and Maynard Smith 1976; Rosenzweig 1981, 1987; Schreiber et al. 2000; Schreiber and Vejdani 2006). Our results demonstrate that environmental stochasticity can reverse or amplify these

We find that environmental stochasticity can partially exorcize the ghost of competition past. Under equilibrium conditions, ideal free competitors occupy only habitat patches in which they are competitively superior (Lawlor and Maynard Smith 1976; Connell 1980; Rosenzweig 1981, 1987). When environmental fluctuations are sufficiently large relative to fitness differences between the competing species, we find that there is selection for competitors occupying patches in which they are competitively inferior—conditional sink populations. Using computer simulations, Schmidt et al. (2000) observed a similar exorcism of the ghost of competition past for discrete-time two-patch models of two competing species. Our results provide an analytical extension of their work to any number of patches and any number of competing species. Moreover, we find that along environmental gradients, environmental stochasticity can select

for several competitors occupying sink habitat patches at the edges of these gradients (i.e., unconditional sink populations). This simultaneous selection for conditional and unconditional sink populations can result in complex species distributions along an environmental gradient (e.g., species disappearing and reappearing along the gradient). Similar complex patterns have been observed along elevational gradients in birds (Noon 1981; Campos-Cerqueira et al. 2017). For example, on Camel's Hump Mountain, the hermit thrush (*Catharus guttatus*) is most common at lower (400 m) and higher (800 m) elevations but is less common at intermediate (600 m) elevations (Noon 1981). Whether environmental fluctuations play a role in these empirical patterns remains to be understood.

Our results highlight how environmental fluctuations can select for enemy-free space in two ways. First, environmental fluctuations in higher-quality habitat may select for prey using lower-quality habitats and thereby create unconditional sink populations. If these lower-quality habitats only support low prey densities and the predators are less sensitive to the environmental fluctuations, then the predators may evolve to occupy only the higher-quality habitat. Thus, the lower-quality habitat becomes enemy-free space. In this case, the spatial bet hedging by the prey creates the enemy-free space. An alternative pathway to enemy-free space occurs when both species are sensitive to the environmental fluctuations and the intensity of these fluctuations vary across the landscape. This spatial variation can select for contrary choices—prey selecting patches with greater risk and predators selecting patches with lower risk. This form of selection for enemy-free space is a stochastic analog of fixed spatial heterogeneity selecting for contrary choices (Fox and Eisenbach 1992; Schreiber et al. 2000, 2002; Schreiber and Vejdani 2006): prey select lower-quality patches to lower the reproductive success of their predators, and predators select high-quality patches to maximize their per capita reproductive success.

Eco-Evolutionary Hydra Effects

Our results on predator-prey coevolution illustrate how environmental stochasticity drive hydra effects over evolutionary time. Named after the mythological beast that grew two heads to replace a lost head, a hydra effect occurs when a population's mean density increases in response to an increase in its per capita mortality rate (Abrams 2009; Sieber and Hilker 2012; Cortez and Abrams 2016). For example, Abrams (2009) found that increasing the per capita mortality rate of a predator with a type II functional response could lead to a long-term increase in the predator's mean density. Similar to increasing per capita mortality rates, increasing environmental stochasticity (σ^2) reduces stochastic per capita growth rates (from μ to $\mu - \sigma^2/2$) and consequently of-

ten has negative impacts on average population densities in the long term (Lande et al. 2003). For example, for Lotka-Volterra predator-prey dynamics with environmental stochasticity, increasing environmental stochasticity experienced by the predator decreases its average density in the long term (May 1975) (see also the mean density \hat{x}_i expressions in the supplemental PDF, sec. S5). However, we find that if there is sufficient time for the patch selection strategies of the predator and prey to evolve to their new coESS, then increasing environmental stochasticity may cause the average predator density to increase (fig. 1D). Intuitively, sufficiently high environmental stochasticity can select for a predator to hedge its bets by occupying an environmentally stable but low-quality patch. This spatial bet hedging lowers the predation pressure on the prey in the source habitat, resulting in an increase of its average density and a corresponding increase in the average predator density. We found similar hydra effects when the prey experiences increasing levels of environmental stochasticity (fig. 1B).

Caveats and Future Directions

To simultaneously confront the complexities of species coevolution in a spatially and temporally variable environment, we made several simplifying assumptions. Relaxing these assumptions provides significant challenges for future research. Most importantly, our framework assumes that species do not assess or respond to temporal changes in habitat quality; they exhibit a fixed spatial distribution. While this assumption is a good first-order approximation frequently made in the theoretical literature (Hassell et al. 1991; van Baalen and Sabelis 1993; Holt 1997; Jansen and Yoshimura 1998; Schmidt et al. 2000; Schreiber et al. 2000; Schreiber and Vejdani 2006; Schreiber 2012), spatial distributions typically vary in time in response to environmental fluctuations. Hence, a major challenge for future work is developing methods to study the evolution of dispersal rates in spatially explicit and temporally variable landscapes. While there has been extensive analytical and numerical work on this question for single species (Levin et al. 1984; McPeek and Holt 1992; Hutson et al. 2001; Ronce 2007; Cantrell and Cosner 2018; Cantrell et al. 2021), much less work exists for interacting species (see, however, Lion et al. 2006; Schreiber and Saltzman 2009; Lion and Gandon 2015).

As most ecological communities reside in spatially and temporally variable environments, we might expect that many of our qualitative predictions occur in nature. However, as noted by Urban et al. (2020), "to date, few empirical studies completely evaluate eco-evolutionary interactions in space through field manipulations, and even fewer test for underlying mechanisms" (p. 17488). Ideally, to test the theory presented here, one would collect data on spatial and temporal variation in species demographic rates, interaction

strengths, and densities over sufficiently long time frames. Alternatively, one could evaluate whether key ingredients of conditions and consequences hold for interacting species occuring over some environmental gradient or patchy landscape. For example, our results predict that greater environmental fluctuations will select for greater range overlap of competing species. Hence, one could attempt a metaanalysis similar to Urban et al. (2020) to evaluate across multiple competitive metacommunities whether such a correlation exists, ideally controlling for the degree of spatial heterogeneity across the landscape. Such analyses could identify whether reciprocal selection among interacting species give rise to some of the outcomes predicted by our theory.

Conclusion

In conclusion, our work provides one theoretical approach to studying how spatial heterogeneity, temporal variation, and species interactions drive the evolution of habitat choice. In this framework, stochastic sink populations are the norm, not the exception, because of species using space to hedge their bets. For antagonistic species interactions, this bet hedging can select for predators seeking refuge in preyfree space and can exorcise the ghost of competition past. We anticipate that applying these methods to models with more species will reveal new surprises.

Acknowledgments

We thank the anonymous reviewers, the associate editor, and the editor for extensive valuable feedback on the manuscript. This work was funded in part by National Science Foundation grants DMS-1716803 to S.J.S., DMS-2147903 to A.H., and DMS-1853467 to D.H.N.

Statement of Authorship

S.J.S. conceived the study with input from A.H. and D.H.N. The mathematical analysis was carried out by A.H., D.H.N., and S.J.S. The R code was written by S.J.S. The manuscript was written by S.J.S. with feedback from A.H. and D.H.N. The supplemental PDF was written by A.H., D.H.N., and S.J.S.

Data and Code Availability

R code to reproduce all results is available on Zenodo (https://doi.org/10.5281/zenodo.7510276; Schreiber 2023).

References

Abrams, P. A. 2009. When does greater mortality increase population size? the long history and diverse mechanisms underlying the hydra effect. Ecology Letters 12:462-474.

- Amarasekare, P., and R. M. Nisbet. 2001. Spatial heterogeneity, source-sink dynamics, and the local coexistence of competing species. American Naturalist 158:572-584.
- Barson, N., J. Cable, and C. Van Oosterhout. 2009. Population genetic analysis of microsatellite variation of guppies (Poecilia reticulata) in Trinidad and Tobago: evidence for a dynamic source-sink metapopulation structure, founder events and population bottlenecks. Journal of Evolutionary Biology 22:485-497.
- Bascompte, J., H. Possingham, and J. Roughgarden. 2002. Patchy populations in stochastic environments: critical number of patches for persistence. American Naturalist 159:128-137.
- Benaïm, M., and S. Schreiber. 2019. Persistence and extinction for stochastic ecological models with internal and external variables. Journal of Mathematical Biology 79:393-431.
- Berdegue, M., J. Trumble, J. Hare, and R. Redak. 1996. Is it enemyfree space? the evidence for terrestrial insects and freshwater arthropods. Ecological Entomology 21:203-217.
- Brown, J., and T. Vincent. 1987. Coevolution as an evolutionary game. Evolution 41:66-79.
- Burner, R., A. Styring, M. Rahman, and F. Sheldon. 2019. Occupancy patterns and upper range limits of lowland Bornean birds along an elevational gradient. Journal of Biogeography 46:2583-
- Campos-Cerqueira, M., W. Arendt, J. Wunderle Jr., and T. Aide. 2017. Have bird distributions shifted along an elevational gradient on a tropical mountain? Ecology and Evolution 7:9914-9924.
- Cantrell, R., and C. Cosner. 2018. Evolutionary stability of ideal free dispersal under spatial heterogeneity and time periodicity. Mathematical Biosciences 305:71-76.
- Cantrell, R., C. Cosner, and K. Lam. 2021. Ideal free dispersal under general spatial heterogeneity and time periodicity. SIAM Journal on Applied Mathematics 81:789-813.
- Chesson, P., and J. Kuang. 2008. The interaction between predation and competition. Nature 456:235-238.
- Chettri, S., S. Bhupathy, and B. K. Acharya. 2010. Distribution pattern of reptiles along an eastern Himalayan elevation gradient, India. Acta Oecologica 36:16-22.
- Childs, D., C. Metcalf, and M. Rees. 2010. Evolutionary bet-hedging in the real world: empirical evidence and challenges revealed by plants. Proceedings of the Royal Society B 277:3055-3064.
- Cohen, D. 1966. Optimizing reproduction in a randomly varying environment. Journal of Theoretical Biology 12:119-129.
- Cole, N., C. Jones, and S. Harris. 2005. The need for enemy-free space: the impact of an invasive gecko on island endemics. Biological Conservation 125:467-474.
- Connell, J. 1980. Diversity and the coevolution of competitors, or the ghost of competition past. Oikos 35:131-138.
- Cortez, M. H., and P. A. Abrams. 2016. Hydra effects in stable communities and their implications for system dynamics. Ecology 97:1135-1145.
- Denno, R., S. Larsson, and K. Olmstead. 1990. Role of enemy-free space and plant quality in host-plant selection by willow beetles. Ecology 71:124-137.
- Diamond, J. 1973. Distributional ecology of New Guinea birds: recent ecological and biogeographical theories can be tested on the bird communities of New Guinea. Science 179:759-769.
- . 1978. Niche shifts and the rediscovery of interspecific competition: why did field biologists so long overlook the widespread evidence for interspecific competition that had already impressed Darwin? American Scientist 66:322-331.

- Dias, P., G. Verheyen, and M. Raymond. 1996. Source-sink populations in Mediterranean blue tits: evidence using single-locus minisatellite probes. Journal of Evolutionary Biology 9:965–978.
- Edwards, K. F., and S. J. Schreiber. 2010. Preemption of space can lead to intransitive coexistence of competitors. Oikos 119:1201–1209.
- Evans, S., A. Hening, and S. J. Schreiber. 2015. Protected polymorphisms and evolutionary stability of patch-selection strategies in stochastic environments. Journal of Mathematical Biology 71:325–359.
- Evans, S. N., P. Ralph, S. J. Schreiber, and A. Sen. 2013. Stochastic growth rates in spatio-temporal heterogeneous environments. Journal of Mathematical Biology 66:423–476.
- Feng, T., C. Li, X. Zheng, S. Lessard, and Y. Tao. 2022. Stochastic replicator dynamics and evolutionary stability. Physical Review E 105:044403.
- Foster, D., and P. Young. 1990. Stochastic evolutionary game dynamics. Theoretical Population Biology 38:219–232.
- Fox, L. R., and J. Eisenbach. 1992. Contrary choices: possible exploitation of enemy-free space by herbivorous insects in cultivates vs. wild crucifers. Oecologia 89:574–579.
- Fretwell, S. D., and H. L. J. Lucas. 1969. On territorial behavior and other factors influencing habitat distribution in birds. Acta Biotheoretica 19:16–36.
- Furrer, R., and G. Pasinelli. 2016. Empirical evidence for sourcesink populations: a review on occurrence, assessments and implications. Biological Reviews 91:782–795.
- Gardiner, C. 2009. Stochastic methods: a handbook for the natural and social sciences. 4th ed. Series in Synergetics. Springer, Berlin.
- Greeney, H., M. Meneses, C. Hamilton, E. Lichter-Marck, R. W. Mannan, N. Snyder, H. Snyder, S. Wethington, and L. Dyer. 2015. Trait-mediated trophic cascade creates enemy-free space for nesting hummingbirds. Science Advances 1:e1500310.
- Hänfling, B., and D. Weetman. 2006. Concordant genetic estimators of migration reveal anthropogenically-enhanced source-sink population structure in the river sculpin, *Cottus gobio*. Genetics 173:1487–1501.
- Hassell, M. P., R. M. May, S. W. Pacala, and P. L. Chesson. 1991. The persistence of host-parasitoid associations in patchy environments.I. A general criterion. American Naturalist 138:568–583.
- Heisswolf, A., E. Obermaier, and H. Poethke. 2005. Selection of large host plants for oviposition by a monophagous leaf beetle: nutritional quality or enemy-free space? Ecological Entomology 30:299–306.
- Hening, A., and D. H. Nguyen. 2018a. Coexistence and extinction for stochastic Kolmogorov systems. Annals of Applied Probability 28:1893–1942.
- 2018b. Persistence in stochastic Lotka-Volterra food chains with intraspecific competition. Bulletin of Mathematical Biology 80:2527–2560.
- ———. 2018c. Stochastic Lotka–Volterra food chains. Journal of Mathematical Biology 77:135–163.
- Hening, A., D. H. Nguyen, and P. Chesson. 2021. A general theory of coexistence and extinction for stochastic ecological communities. Journal of Mathematical Biology 82:1–76.
- Hofbauer, J., and K. Sigmund. 1998. Evolutionary games and population dynamics. Cambridge University Press, Cambridge.
- Holt, R. D. 1977. Predation, apparent competition and the structure of prey communities. Theoretical Population Biology 12:197–229.
- ——. 1985. Patch dynamics in two-patch environments: some anomalous consequences of an optimal habitat distribution. Theoretical Population Biology 28:181–208.

- . 1997. On the evolutionary stability of sink populations. Evolutionary Ecology 11:723–731.
- Hutson, V., K. Mischaikow, and P. Poláčik. 2001. The evolution of dispersal rates in a heterogeneous time-periodic environment. Journal of Mathematical Biology 43:501–533.
- Jansen, V. A. A., and J. Yoshimura. 1998. Populations can persist in an environment consisting of sink habitats only. Proceeding of the National Academy of Sciences of the USA 95:3696–3698.
- Jeffries, M. J., and J. H. Lawton. 1984. Enemy-free space and the structure of ecological communities. Biological Journal of the Linnean Society 23:269–286.
- Jonzén, N., C. Wilcox, and H. Possingham. 2004. Habitat selection and population regulation in temporally fluctuating environments. American Naturalist 164:103–103.
- Kadmon, R., and K. Tielbörger. 1999. Testing for source-sink population dynamics: an experimental approach exemplified with desert annuals. Oikos 86:417–429.
- Kaminski, L., A. Freitas, and P. Oliveira. 2010. Interaction between mutualisms: ant-tended butterflies exploit enemy-free space provided by ant-treehopper associations. American Naturalist 176:322–334.
- Keagy, J., S. J. Schreiber, and D. A. Cristol. 2005. Replacing sources with sinks: when do populations go down the drain? Restoration Ecology 13:529–535.
- Kisdi, E. 2002. Dispersal: risk spreading versus local adaptation. American Naturalist 159:579–596.
- Kreuzer, M., and N. Huntly. 2003. Habitat-specific demography: evidence for source-sink population structure in a mammal, the pika. Oecologia 134:343–349.
- Křivan, V., R. Cressman, and C. Schneider. 2008. The ideal free distribution: a review and synthesis of the game-theoretic perspective. Theoretical Population Biology 73:403–425.
- Lande, R., S. Engen, and B. Sæther. 2003. Stochastic population dynamics in ecology and conservation: an introduction. Oxford University Press, Oxford.
- Law, R., and R. D. Morton. 1996. Permanence and the assembly of ecological communities. Ecology 77:762–775.
- Lawlor, L., and J. Maynard Smith. 1976. The coevolution and stability of competing species. American Naturalist 110:79–99.
- Levin, S. A., D. Cohen, and A. Hastings. 1984. Dispersal strategies in patchy environments. Theoretical Population Biology 26:165–191.
- Lion, S., and S. Gandon. 2015. Evolution of spatially structured hostparasite interactions. Journal of Evolutionary Biology 28:10–28.
- Lion, S., M. Van Baalen, and W. Wilson. 2006. The evolution of parasite manipulation of host dispersal. Proceedings of the Royal Society B 273:1063–1071.
- Loreau, M., T. Daufresne, A. Gonzalez, D. Gravel, F. Guichard, S. Leroux, N. Loeuille, F. Massol, and N. Mouquet. 2013. Unifying sources and sinks in ecology and earth sciences. Biological Reviews 88:365–379.
- Manier, M., and S. Arnold. 2005. Population genetic analysis identifies source–sink dynamics for two sympatric garter snake species (*Thamnophis elegans* and *Thamnophis sirtalis*). Molecular Ecology 14:3965–3976.
- Markowitz, H. M. 1952. Portfolio selection. Journal of Finance 7:77–91.———. 1991. Foundations of portfolio theory. Journal of Finance 46:469–477.
- . 2010. Portfolio theory: as I still see it. Annual Review of Financial Economics 2:1–23.
- May, R. M. 1973. Stability in randomly fluctuating versus deterministic environments. American Naturalist 107:621–650.

- -. 1975. Stability and complexity in model ecosystems. 2nd ed. Princeton University Press, Princeton, NJ.
- McDowall, R. 2010. Why be amphidromous: expatrial dispersal and the place of source and sink population dynamics? Reviews in Fish Biology and Fisheries 20:87-100.
- McPeek, M., and R. D. Holt. 1992. The evolution of dispersal in spatially and temporally varying environments. American Naturalist 6:1010-1027.
- Monson, D., D. Doak, B. Ballachey, and J. Bodkin. 2011. Could residual oil from the Exxon Valdez spill create a long-term population "sink" for sea otters in Alaska? Ecological Applications 21:2917-
- Morris, D. W. 2003. Toward an ecological synthesis: a case for habitat selection. Oecologia 136:1-13.
- -. 2011. Adaptation and habitat selection in the ecoevolutionary process. Proceedings of the Royal Society B 278:2401-2411.
- Murphy, S. 2004. Enemy-free space maintains swallowtail butterfly host shift. Proceedings of the National Academy of Sciences 101:18048-18052.
- Murphy, S., J. Lill, M. Bowers, and M. Singer. 2014. Enemy-free space for parasitoids. Environmental Entomology 43:1465-1474.
- Nolting, B. C., and K. C. Abbott. 2016. Balls, cups, and quasipotentials: quantifying stability in stochastic systems. Ecology 97:850-864.
- Noon, B. 1981. The distribution of an avian guild along a temperate elevational gradient: the importance and expression of competition. Ecological Monographs 51:105-124.
- Oksanen, T., M. Power, and L. Oksanen. 1995. Ideal free habitat selection and consumer-resource dynamics. American Naturalist 146:565-585.
- Oksendal, B. 2013. Stochastic differential equations: an introduction with applications. Springer, Berlin.
- Polis, G. A., and R. D. Holt. 1992. Intraguild predation: the dynamics of complex trophic interactions. Trends in Ecology and Evolution 7:151-154.
- Pulliam, H. R. 1988. Sources, sinks, and population regulation. American Naturalist 132:652-661.
- Pulliam, H. R., and B. J. Danielson. 1991. Sources, sinks and habitat selection: a landscape perspective on population dynamics. American Naturalist 137:S50-S66.
- Rand, D. A., H. B. Wilson, and J. M. McGlade. 1994. Dynamics and evolution: evolutionary stable attractors, invasion exponents and phenotype dynamics. Philosophical Transactions of the Royal Society B 343:261-283.
- Robinson, H., R. Wielgus, H. Cooley, and S. Cooley. 2008. Sink populations in carnivore management: cougar demography and immigration in a hunted population. Ecological Applications 18:1028-1037.
- Rohr, R., S. Saavedra, G. Peralta, C. M. Frost, L.-F. Bersier, J. Bascompte, and J. Tylianakis. 2016. Persist or produce: a community trade-off tuned by species evenness. American Naturalist 188:411-422.
- Ronce, O. 2007. How does it feel to be like a rolling stone? ten questions about dispersal evolution. Annual Review of Ecology and Systematics 38:231-253.
- Rosenzweig, M. 1981. A theory of habitat selection. Ecology 62:327-335.
- -. 1987. Habitat selection as a source of biological diversity. Evolutionary Ecology 1:315-330.

- -. 1991. Habitat selection and population interactions: the search for mechanism. American Naturalist 137:S5-S28.
- Roughgarden, J. 1979. Theory of population genetics and evolutionary ecology. Macmillan, New York.
- Rowe, C., W. Hopkins, and V. Coffman. 2001. Failed recruitment of southern toads (Bufo terrestris) in a trace element-contaminated breeding habitat: direct and indirect effects that may lead to a local population sink. Archives of Environmental Contamination and Toxicology 40:399-405.
- Roy, H., L. Handley, K. Schönrogge, R. Poland, and B. Purse. 2011. Can the enemy release hypothesis explain the success of invasive alien predators and parasitoids? BioControl 56:451-468.
- Rubinstein, M. 2002. Markowitz's "portfolio selection": a fifty-year retrospective. Journal of Finance 57:1041-1045.
- Schmidt, K., J. Earnhardt, J. Brown, and R. Holt. 2000. Habitat selection under temporal heterogeneity: exorcizing the ghost of competition past. Ecology 81:2622-2630.
- Schreiber, S. J. 2012. Evolution of patch selection in stochastic environments. American Naturalist 180:17-34.
- -. 2023. R code from: Coevolution of patch selection in stochastic environments. American Naturalist, Zenodo, https:// doi.org/10.5281/zenodo.7510276.
- Schreiber, S. J., M. Benaïm, and K. A. S. Atchadé. 2011. Persistence in fluctuating environments. Journal of Mathematical Biology 62:655-683.
- Schreiber, S. J., L. R. Fox, and W. M. Getz. 2000. Coevolution of contrary choices in host-parasitoid systems. American Naturalist 155:637-648.
- -. 2002. Parasitoid sex allocation affects coevolution of patch selection in host-parasitoid systems. Evolutionary Ecology Research 4:701-718.
- Schreiber, S. J., S. Patel, and C. terHorst. 2018. Evolution as a coexistence mechanism: does genetic architecture matter? American Naturalist 191:407-420.
- Schreiber, S. J., and E. Saltzman. 2009. Evolution of predator and prey movement into sink habitats. American Naturalist 174:68-81.
- Schreiber, S. J., and M. Vejdani. 2006. Handling time promotes the coevolution of aggregation in predator-prey systems. Proceedings of the Royal Society B 273:185-191.
- Sieber, M., and F. M. Hilker. 2012. The hydra effect in predatorprey models. Journal of Mathematical Biology 64:341-360.
- Soetaert, K., T. Petzoldt, and R. Setzer. 2010. Solving differential equations in R: package deSolve. Journal of Statistical Software 33:1-25.
- Stearns, S. C. 2000. Daniel Bernoulli (1738): evolution and economics under risk. Journal of Biosciences 25:221-228.
- Tittler, R., L. Fahrig, and M. Villard. 2006. Evidence of large-scale source-sink dynamics and long-distance dispersal among Wood Thrush populations. Ecology 87:3029-3036.
- Turelli, M. 1977. Random environments and stochastic calculus. Theoretical Population Biology 12:140-178.
- -. 1978. A reexamination of stability in randomly varying versus deterministic environments with comments on the stochastic theory of limiting similarity. Theoretical Population Biology 13:244–267.
- 1986. Stochastic community theory: a partially guided tour. Pages 321-339 in T. G. Hallam and S. A. Levin, eds. Mathematical ecology. Springer, Berlin.
- Turelli, M., and J. H. Gillespie. 1980. Conditions for the existence of stationary densities for some two-dimensional diffusion processes with applications in population biology. Theoretical Population Biology 17:167-189.

Urban, M. C., S. Y. Strauss, F. Pelletier, E. P. Palkovacs, M. A. Leibold, A. P. Hendry, L. De Meester, S. M. Carlson, A. L. Angert, and S. T. Giery. 2020. Evolutionary origins for ecological patterns in space. Proceedings of the National Academy of Sciences of the USA 117:17482–17490.

van Baalen, M., and M. W. Sabelis. 1993. Coevolution of patch selection strategies of predator and prey and the consequences for ecological stability. American Naturalist 142:646–670.

Vierling, K. T. 2000. Source and sink habitats of red-winged blackbirds in a rural/suburban landscape. Ecological Applications 10:1211–1218.

Watkinson, A., and W. Sutherland. 1995. Sources, sinks and pseudosinks. Journal of Animal Ecology 64:126–130.

Zivot, E. 2017. Introduction to computational finance and financial econometrics. Chapman & Hall/CRC, Boca Raton, FL.

References Cited Only in the Online Enhancements

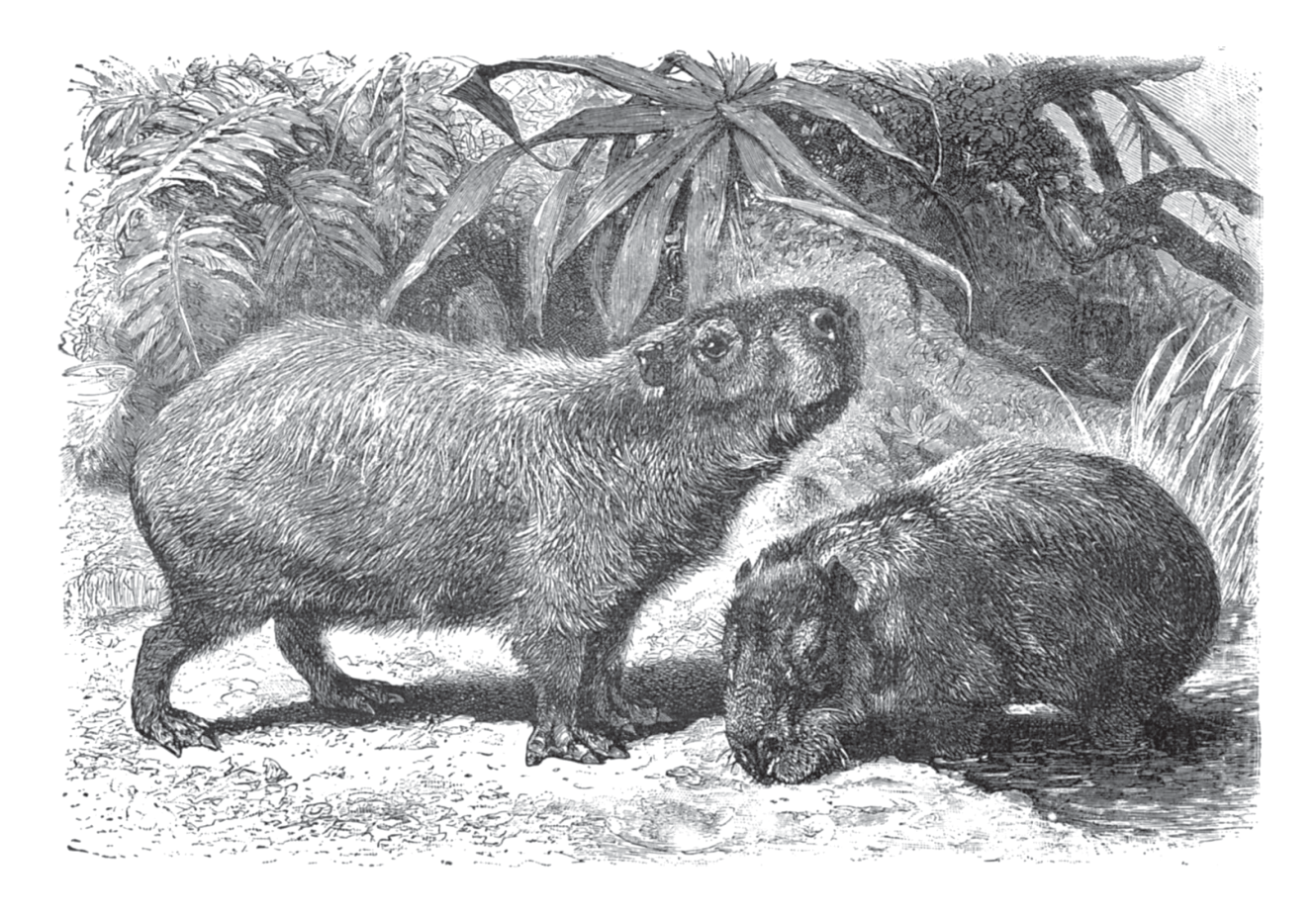
Benaïm, M. 2018. Stochastic persistence. arXiv, https://doi.org/10.48550/arXiv.1806.08450.

Benaïm, M., and C. Lobry. 2016. Lotka–Volterra with randomly fluctuating environments or "how switching between beneficial environments can make survival harder." Annals of Applied Probability 26:3754–3785.

Chesson, P. L. 1982. The stabilizing effect of a random environment. Journal of Mathematical Biology 15:1–36.

Hofbauer, J. 1981. A general cooperation theorem for hypercycles. Monatshefte für Mathematik 91:233–240.

> Associate Editor: Christopher A. Klausmeier Editor: Jennifer A. Lau



"The accompanying illustration of that strange animal the Capybara, the 'native hog' of South America, the largest of existing rodents, will give an idea of the kind of illustrations used in the numbers we have thus far received." From the review of *Our Living World* by Selmar Hess (*The American Naturalist*, 1885, 19:780).